

# Stabilizing boundary time crystals through Non-markovian dynamics

Bandita Das,<sup>1</sup> Rahul Ghosh,<sup>1</sup> and Victor Mukherjee<sup>1</sup>

<sup>1</sup>*Department of Physical Sciences, Indian Institute of Science Education and Research Berhampur, Berhampur 760010, India*  
(Dated: August 14, 2025)

We study Boundary time crystals (BTCs) in the presence of non-Markovian dynamics. In contrast to BTCs observed in earlier works in the Markovian regime, we show that non-Markovian dynamics can be highly beneficial for stabilizing BTCs over a wide range of parameter values, even in the presence of intermediate rates of dissipation. We analyze the effect of non-Markovian dynamics on BTCs using quantum Fisher information, order parameter, a measure of non-Markovianity, and a dynamical phase diagram, all of which show complex behaviours with changing non-Markovianity parameters. Our studies can pave the way for stabilizing time crystals in dissipative systems, as well as lead to studies on varied dissipative dynamics on time translational symmetry breaking.

## I. INTRODUCTION

The dynamics of many-body quantum systems driven out of equilibrium is a major field of theoretical [1, 2] and experimental [3] research. Specifically, several open questions remain regarding thermalisation in driven quantum systems, which is in turn connected to a relatively newly discovered non-equilibrium phase of matter - viz. time crystals, which are formed in the presence of spontaneous time-translational symmetry breaking (TTSB). Discrete time crystals are formed in quantum systems driven periodically in time [4–8], while continuous or boundary time crystals (BTCs) are associated with limit cycles in open quantum systems in the presence of time-independent Hamiltonians [9–11]. Interestingly, dissipative discrete time crystals have been shown to be related to quantum engines [5], while BTCs can be a prime candidate for the development of many-body autonomous engines [12]. In addition, use of time crystals to model qubits for quantum processing tasks has also been proposed [13]. On the fundamental side, the thermodynamics of time crystals has received significant attention lately [14]. Consequently, finding methods of generating and stabilizing time-crystals in varied many-body systems is a crucial question in this field. This becomes even more pertinent due to the fact that while weak dissipation has been shown to favour the existence of time crystals [15–19], strong dissipation can have a detrimental effect on the same, for discrete time crystals [16, 20, 21] as well as for BTCs [9, 22, 23].

Most of the works on time crystals in open quantum systems have focused on Markovian dynamics. On the other hand, non-Markovian dynamics, which may arise due to strong coupling or comparable dimensions of system and bath, may become an inescapable phenomenon in realistic systems [24]. Therefore, studying the fate of time crystals in the presence of non-Markovian dynamics is an important open question. Notably, the intriguing question remains if information backflow associated with non-Markovian dynamics can be harnessed to increase the stability of time crystals in the presence of strong dissipation. Recently, it was shown that non-Markovian dynamics can be significantly beneficial for stabilizing dis-

crete time crystals in the presence of intermediate rates of dissipation, in the semi-classical limit [21]. However, whether the benefits of non-Markovian dynamics extend to BTCs as well is an open question, which we address in this work. As we discuss below, non-Markovian dynamics can indeed allow the existence of BTCs in the presence of intermediate rates of dissipation, as compared to Markovian dynamics, which can support BTCs only for weak rates of dissipation. We support our analysis using quantum Fisher information (QFI) and an order parameter, both of which show interesting characteristics associated with the BTC to non-BTC phase transition. In addition, we also use a measure of non-Markovianity  $\mathcal{N}$  to show that intermediate values of  $\mathcal{N}$  can be specially beneficial for the generation of BTCs. Finally, we summarize our results using a phase diagram which shows the behavior of BTCs for different strengths of non-Markovianity and rates of dissipation.

We describe the model and dynamics of the dissipative BTC considered here in Sec. II A, focus on the non-Markovian regime in Sec. II B, discuss QFI in Sec. II C, study the behaviour of an order parameter in Sec. II D, analyze the BTC with respect to the measure of non-Markovianity  $\mathcal{N}$  in Sec. II E, and show a complete phase diagram in Sec. II F. Finally, we conclude in Sec. III.

## II. MODEL AND DYNAMICS

### A. Dissipative Boundary time crystals

BTCs are associated with the continuous spontaneous breaking of time translational symmetry. We consider the setup introduced in Refs. [9, 25]; the system considered here comprises  $N_b$  driven two-level spins, termed as the boundary, that are collectively coupled to a Bosonic field mode comprising the bulk of the setup. Under the Markovian approximation, the system represented by the collective spin degrees of freedom evolves according to a time-independent Gorini-Kossakowski-Lindblad-Sudarshan master equation, where coherent Hamiltonian driving competes with collective spin decay [24]. At sufficiently strong coherent driving, the mag-

netisation exhibits oscillatory behaviour, with its lifetime increasing indefinitely as the number of spins grows. While finite-size systems eventually settle into a stationary equilibrium value, in the thermodynamic limit, these oscillations persist indefinitely, signalling the spontaneous breaking of continuous time-translation symmetry. Moreover, in the BTC phase, the collective dynamics form closed periodic orbits that characterise the system's long-term evolution.

The many-body system is described by the time-independent Hamiltonian which is given by [9]

$$H_b = \omega_0 \hat{S}_x + \frac{\omega_x}{S} (\hat{S}_x)^2 + \frac{\omega_z}{S} (\hat{S}_z)^2. \quad (1)$$

Here  $\hat{S}_\mu = \frac{1}{2} \sum_k \hat{\sigma}_\mu^k$  represents collective spin degrees of freedom,  $\hat{\sigma}_\mu^k (\mu = x, y, z)$  are the Pauli matrices acting on the  $k$ -th spin,  $\omega_0$  is the frequency of the two level system and we consider  $\omega_x = 0, \omega_z = 0$  in the main text. The Lindblad equation describing the evolution of the state  $\hat{\rho}_b$  of the system is given by [26, 27]

$$\frac{d\hat{\rho}_b}{dt} = i[\hat{\rho}_b, \hat{H}_b] + \frac{\kappa(t)}{S} (\hat{S}_- \hat{\rho}_b \hat{S}_+ - \frac{1}{2} \{ \hat{S}_+ \hat{S}_-, \hat{\rho}_b \}). \quad (2)$$

In the above equation (2),  $\hat{S}_\pm$  are the raising and lowering operators i.e.  $\hat{S}_\pm = \hat{S}_x \pm i\hat{S}_y$  and we fix the total spin  $S = N_b/2$ . In order to study the effect of non-Markovian dynamics on the behavior of BTC, we consider a phenomenological model analogous to the Jaynes-Cummings model describing the decay of a two-level system coupled to Bosonic modes with a Lorentzian spectral function [24]. To this end, we assume a  $\kappa(t)$  of the form

$$\kappa(t) = \begin{cases} \frac{2m\kappa_0 \sinh(td/2)}{d \cosh(td/2) + m \sinh(td/2)} & |\kappa(t)| < \kappa_{max} \\ \kappa_{max} & |\kappa(t)| \geq \kappa_{max}, \end{cases} \quad (3)$$

where  $m$  denotes the spectral width of the bath, while  $\kappa_0$  is related to the Markovian system-bath coupling strength, and  $d = \sqrt{m^2 - 2m\kappa_0}$ , frequency of decay rate  $\omega_d = d/2$ .  $\kappa_{max} > \kappa_0$  is a parameter which can be tuned to control the maximum possible rate of dissipation, while in the case of the damped Jaynes-Cummings model,  $\kappa_{max} \rightarrow \infty$ . The above form of  $\kappa(t)$  (Eq. (3)) allows us to tune between the Markovian regime ( $m > 2\kappa_0$ ) in which case  $\kappa(t) > 0 \forall t$  and  $\kappa(t \rightarrow \infty) = \frac{2\kappa_0 m}{d+m}$ , and the non-Markovian regime ( $m < 2\kappa_0$ ), in which case  $\kappa(t)$  assumes an oscillatory form realized by replacing  $\sinh$  ( $\cosh$ ) by  $\sin$  ( $\cos$ ) in Eq. (3), and can take negative values for some time interval [28]. Here complete positivity is ensured by  $\int_0^t \kappa(t) dt \geq 0$  for all  $t$  [29, 30]. We work in the thermodynamic limit  $N_b \rightarrow \infty$ , where the spins are in a product state, and semi-classical analysis suffices to study this model (see Appendix A) and we solve the semi-classical equation of motion (A2). We emphasize that in spite of the phenomenological form of  $\kappa(t)$ , the time-local form of the master equation (2) and the ability of tune continuously between the Markovian and the non-Markovian regime makes this model an ideal platform for

understanding the role of non-Markovian dynamics and information backflow on the fate of BTCs; furthermore, the Jaynes-Cummings model (cf. Eq. (3)) has also been realized experimentally in optical cavity setups [31].

BTCs were realised in the above model (2) for a Markovian dissipative environment with a time-independent rate of dissipation ( $m \gg \kappa_0$ ;  $\kappa(t) = \kappa_0 > 0 \forall t$ ), where persistent oscillations were shown by the  $m_z = S_z/S$  in the thermodynamic limit, for small  $\kappa_0$  ( $\frac{\omega_0}{\kappa_0} > 1$ ) [9]. On the other hand, stronger rates of dissipation ( $\frac{\omega_0}{\kappa_0} < 1$ ) result in replacement of the BTC phase by a time-independent steady state (TISS) (see Fig. 1a). In the next section, we tune the value of  $m/\kappa_0$  from  $m \gg \kappa_0$  to  $m < \kappa_0$ , to study the behaviour of the system in both the Markovian ( $m > 2\kappa_0$ ), as well as the non-Markovian ( $m < 2\kappa_0$ ) regime. We have set  $\kappa_0 = 1$  for all the numerical results shown here.

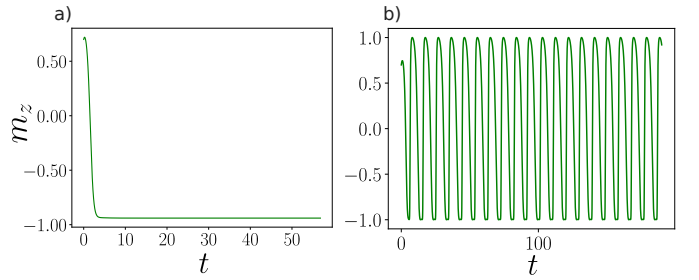


FIG. 1. Plot showing the dynamics of  $m_z$  in the (a) Markovian ( $\kappa(t) = \kappa_0 \forall t$ ) and the (b) non-Markovian ( $m = \kappa_0/4$ ) regime, for  $\omega_0/\kappa_0 = 0.3$ , and  $\kappa_0 = 1$ . As shown here, the Markovian regime results in a time-independent steady state, while the non-Markovian regime is associated with a BTC phase.

For the sake of completeness we also study the effect of non zero  $\omega_x$  and  $\omega_z$  in Appendix B and Fig. 6.

## B. Non-Markovian regime

In this section we focus on the non-Markovian regime ( $m < 2\kappa_0$ ), characterized by a periodically varying  $\kappa(t)$  assuming negative values for some time intervals (see Eq. (3)), and associated with the so called information back-flow [32]. In contrast to the behavior reported for Markovian dynamics [9] where BTC phase is present only for  $\frac{\omega_0}{\kappa_0} > 1$ , numerical analysis shows that non-Markovian dynamics makes BTCs significantly more robust against higher values of  $\kappa_0$ , as signified by the presence of time-crystalline order in the limit of  $\frac{\omega_0}{\kappa_0} < 1$  and finite  $\kappa_{max} > \kappa_0$  (see Fig. 1). This robustness of the BTC phase w.r.t.  $\kappa_0$  suggests the beneficial role played by information backflow in stabilizing time-crystalline order in the presence of intermediate rates of dissipation [30, 33]. We study the behavior for different values of  $\omega_0$  in Fig. 2. Small values of  $\omega_0$  are associated with a non-BTC phase, characterized by irregular oscillations of  $m_z$

w.r.t. time  $t$  (see Fig. 2a), which correspond to spurious peaks in the corresponding FFT for different frequencies  $\omega$  (see Fig. 2d), and irregular trajectories in the Bloch sphere (see Fig. 2g). As we increase  $\omega_0$ , we obtain a BTC phase for intermediate values of  $\omega_0$ , as shown by persistent oscillations in  $m_z$  (see Fig. 2b), a dominant peak in the FFT (see Fig. 2e), and a limit cycle on the Bloch sphere (see Fig. 2g). Interestingly, as we increase  $\omega_0$  further, we get higher order limit cycles (HO-LC) (see Fig. 2c), supported by multiple dominant Fourier peaks (Fig. 2f)) and a limit cycle on the Bloch sphere (Fig. 2i)).

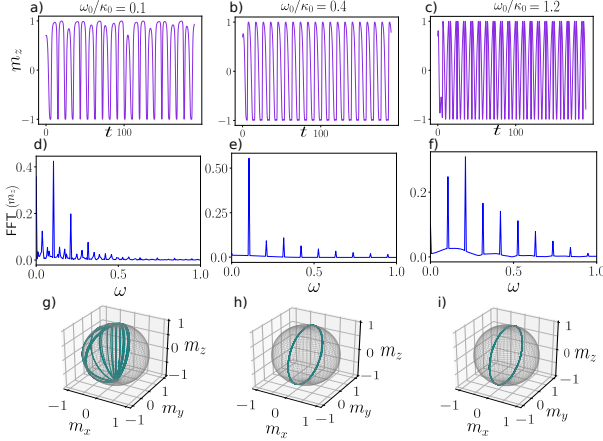


FIG. 2. Plot showing the dynamics of  $m_z$  in the non-Markovian regime for  $m = \kappa_0/4$ , (a, b, c), the corresponding FFT (d, e, f) and the representation of the dynamics on the Bloch sphere (g, h, i), for different values of  $\omega_0/\kappa_0$ , in the non-Markovian regime.  $m_z$  shows (a) irregular oscillations with (b) multiple spurious peaks in the FFT and (c) an irregular trajectory on the Bloch sphere for small  $\omega_0/\kappa_0$ . A moderate value of  $\omega_0/\kappa_0$  is associated with a BTC phase, characterized by (d) an oscillatory  $m_z$  with (e) a dominant frequency in the FFT and (f) a limit cycle on the Bloch sphere. A higher value of  $\omega_0/\kappa_0$  results in (g)  $m_z$  showing oscillations with (h) multiple frequencies and (i) a limit cycle on the Bloch sphere.

### C. Quantum Fisher Information

In this section, we analyse the transition between the BTC and non-BTC phases using quantum Fisher information (QFI). QFI has been widely used for studying the sensitivity of quantum probes [34, 35], and also for detecting quantum phase transitions through divergences in QFI [36]. Here we compute the QFI for various values of  $\omega_0$ , in order to check the BTC to non-BTC transition in this model. In order to calculate the QFI, we first evaluate the density matrix within the mean-field approximation. Following Ref. [37], we write the total density matrix  $\hat{\rho}_b = \hat{\rho}_{\text{MF},\omega_0}$ , for  $N_b$  two-level systems, in a factorized form as

$$\hat{\rho}_{\text{MF},\omega_0} = \bigotimes_{i=1}^{N_b} \hat{\rho}_{i,\omega_0}, \quad (4)$$

where  $\hat{\rho}_{i,\omega_0}$  denotes the reduced density matrix for the  $i$ -th spin. These reduced states are identical for all spins and can be represented in terms of the total spin observables as [38]

$$\hat{\rho}_{i,\omega_0} = \frac{1}{2}(\hat{\mathbb{I}}_2 + m_x \hat{\sigma}^x + m_y \hat{\sigma}^y + m_z \hat{\sigma}^z) \quad (5)$$

where  $\hat{\mathbb{I}}_2$  is the Identity matrix and  $m_\mu = \frac{\langle S_\mu \rangle}{S}$ ,  $\mu \in \{x, y, z\}$ , after taking into account that the system is in a separable state, and  $\mathcal{F}(\hat{\rho}_A \otimes \hat{\rho}_B) = \mathcal{F}(\hat{\rho}_A) + \mathcal{F}(\hat{\rho}_B)$  for any two states  $\hat{\rho}_A$  and  $\hat{\rho}_B$ , we get the total QFI by adding up the QFI  $\mathcal{F}(\hat{\rho}_{i,\omega_0})$  of the reduced state of each qubit, such that [36, 37]

$$\begin{aligned} \mathcal{F}(\hat{\rho}_{\text{MF},\omega_0}) &= N_b \mathcal{F}(\hat{\rho}_{i,\omega_0}) \\ &= N_b \left( 8 \lim_{\delta\omega_0 \rightarrow 0} \frac{(1 - \mathbb{F}(\hat{\rho}_{i,\omega_0 - \delta\omega_0}, \hat{\rho}_{i,\omega_0 + \delta\omega_0}))}{(2\delta\omega_0)^2} \right), \end{aligned} \quad (6)$$

where  $\mathbb{F}(\hat{\rho}_1, \hat{\rho}_2) = \text{Tr} \left[ \sqrt{\sqrt{\hat{\rho}_1} \hat{\rho}_2 \sqrt{\hat{\rho}_1}} \right]$  denotes the fidelity between two density matrices  $\hat{\rho}_1$  and  $\hat{\rho}_2$ , and  $\delta\omega_0$  denotes an infinitesimal change in  $\omega_0$ .

In general phase transitions are associated with divergences in QFI, owing to large changes in the state of a system for a small change in the Hamiltonian parameters. As shown in Fig. 3, the behavior of the QFI suggests a non-BTC to BTC phase transition at  $\omega_0/\kappa_0 \approx 0.15$ , thus showing a significant advantage as compared to Markovian dynamics, where the corresponding phase transition occurs at  $\omega_0/\kappa_0 \approx 1$  for  $m \gg \kappa_0$  (see Ref. [9]). The QFI remains close to zero for large  $\omega_0/\kappa_0$ , which corresponds to BTC and HO-LC phases (see Fig. 2). In contrast, the QFI shows multiple peaks for  $\omega_0/\kappa_0 \lesssim 0.15$ , which can be associated with the irregular dynamics shown in Fig. 2a. For very small  $\omega_0/\kappa_0$ , the dissipation dominates the dynamics, and takes the system to a non-BTC oscillatory state, characterized by a non-limit cycle trajectory on the Bloch sphere (see Appendix C Fig. 7).

### D. Order parameter

In order to gain insight into the transition from an alternative viewpoint, we follow the approach of Ref. [39], where the authors introduce the time-averaged magnetization as an order parameter which is defined as

$$\mu(\omega_0) = \frac{1}{T} \int_0^T m_z(\omega_0, t) dt. \quad (7)$$

Their analysis demonstrates that the time-averaged magnetization exhibits distinct scaling behavior with respect to the relevant system parameter in the two regimes: the steady state phase and the limit-cycle oscillations. Here we plot  $\mu(\omega_0)$  as a function of  $\frac{\omega_0}{\kappa_0}$  in Fig. 3b. While our system in general maintains a non-zero magnetization in

all phases (in contrast to Ref. [39]), it nevertheless reproduces one key feature: a clear difference in the behavior of  $\mu$  in the BTC and non-BTC regimes, separated by a transition at  $\omega_0/\kappa_0 \approx 0.15$ . In the non-BTC regime,  $m_z$  exhibits oscillations ((see Appendix C, Fig. 7)) predominantly on the negative side for  $\frac{\omega_0}{\kappa_0} \rightarrow 0$ , thereby giving rise to a negative  $\mu$ . The irregular dynamics in  $m_z$  (see Fig. 2a) is reflected in a similar irregular but positive behavior of  $\mu$  as well in Fig. 3b, for small but finite values of  $\omega_0/\kappa_0$ . Symmetric oscillations in the BTC regime result in small values of  $\mu$ . However, as we transition into the HO-LC regime, the oscillation frequency gradually changes, and small kink-like features begin to emerge, particularly on the negative side of the  $m_z$  trajectory (see Fig. 2c). As a result,  $\mu$  starts to deviate from zero and tends towards negative values in this regime, reflecting the asymmetry and complexity of the oscillations. Numerical analysis suggests the system stays in the HO-LC phase with varying periods of oscillations for larger values of  $\omega_0$ . Notably, a similar nature of order parameter has been observed in Ref. [40].

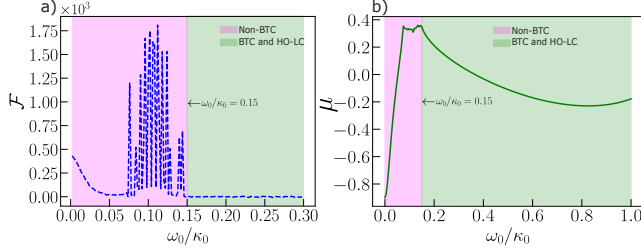


FIG. 3. (a) We plot the QFI in the non-Markovian regime for  $m = \kappa_0/4$ , as a function of  $\omega_0/\kappa_0$ . The transition between the BTC phase and the non-BTC phase is associated with divergences in QFI for  $\omega_0/\kappa_0 \lesssim 0.15$ . (b) We plot the order parameter  $\mu$  as a function of  $\omega_0/\kappa_0$ . BTC to non-BTC transition at  $\omega_0/\kappa_0$  is associated with distinct changes in the behaviour of  $\mu$ .

### E. Non-Markovian Measure

One crucial question in the field of time crystals is, whether a clear relation exists between the existence of a BTC phase and the degree of non-Markovianity present in the dynamics. To this end, we quantify the non-Markovianity using a decay-rate-based measure introduced in Refs. [41, 42]. Specifically, we define a function

$$f(t) = \max(-\kappa(t), 0). \quad (8)$$

This function is identically zero for all times if and only if the system's evolution is Markovian ( $\kappa(t) \geq 0 \forall t$ ); on the other hand a negative  $\kappa(t)$  results in  $f(t) = |\kappa(t)|$ . Hence, any deviation from zero directly signals the presence of non-Markovian dynamics. A cumulative measure of non-Markovianity can thus be constructed via the time

integral [42]

$$\mathcal{N} = \int f(t) dt. \quad (9)$$

A nonzero value of  $\mathcal{N}$  implies that the decay rate  $\kappa(t)$  becomes negative during certain intervals of time, signaling a temporary reversal of information flow from the environment back to the system [26, 43].

To characterize the dynamical phases, we consider the ratio between the amplitude of the dominant frequency peak and the amplitude of the second-largest peak in the FFT of  $m_z$ , here termed as the FFT peak ratio. High values of FFT peak ratio indicates the presence of a BTC phase, while low values correspond to HO-LC or irregular non-BTC phases (see also Fig. 2). We plot the FFT peak ratio as a function of the non-Markovianity measure  $\mathcal{N}$  in Fig. 4 which is calculated by changing the spectral width  $m$  (see Fig. 5). For small values of  $\mathcal{N}$ , the peak ratio exhibits significant fluctuations, indicating an irregular non-BTC phase. As  $\mathcal{N}$  increases, the peak ratio reaches a maximum and remains approximately constant within the BTC regime. Beyond this region, as the system transitions into the higher-order limit cycle (HO-LC) regime, the peak ratio gradually decreases, reflecting the emergence of more complex dynamical structures with multiple competing frequencies. Therefore our results emphasize the importance of information-backflow for the generation of limit cycles, in the form of BTCs for intermediate values of  $\mathcal{N}$ , and as HO-LCs for higher values of  $\mathcal{N}$ .

### F. Phase diagram

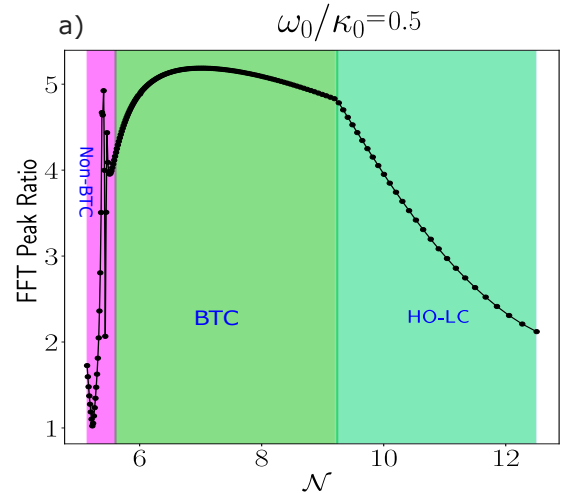


FIG. 4. FFT peak ratio as a function of  $\mathcal{N}$  for a constant  $\frac{\omega_0}{\kappa_0} = 0.5$ . For small  $\mathcal{N}$ , the system does not exhibit the BTC phase, the ratio remains constant, whereas in the HO-LC phase, it decreases due to the presence of multiple comparable dominant frequencies.



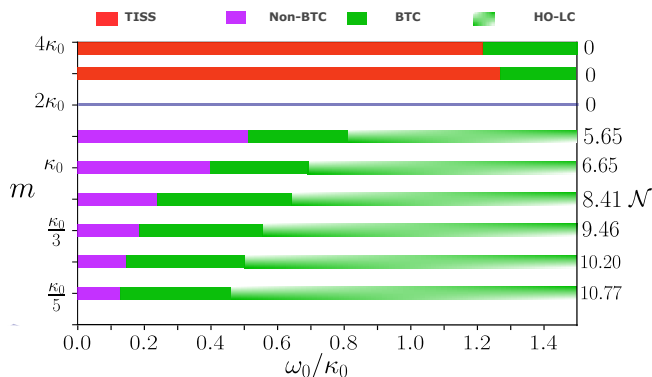


FIG. 5. Complete phase diagram as we go from Markovian to Non-Markovian regime for as functions of  $m$  and  $\mathcal{N}$ . Here  $\kappa_0 = 1$ , and the transition line separating the Markovian and the non-Markovian regimes is shown by the solid line at  $m = 2\kappa_0$ .

The qualitative behaviors of the system across the Markovian and non-Markovian regimes are summarized in the phase diagram shown in Fig. 5. By fixing the dissipation rate  $\kappa_0$ , we traverse between the Markovian regime ( $m > 2\kappa_0$ ) and the non-Markovian regime ( $m < 2\kappa_0$ ) by tuning the parameter  $m$ . This transition is clearly reflected in the system's dynamical response, as illustrated by the stark contrast observed on either side of  $m = 2\kappa_0$  (shown by the black line in Fig. 5).

In the Markovian regime the system tends toward a time independent steady state in the limit of  $\kappa_0 \gg \omega_0$ ; here the time crystalline behavior is suppressed by strong, memoryless dissipation. On the other hand, a BTC phase appears for  $\omega_0 \gtrsim \kappa(t \rightarrow \infty)$ . Upon crossing into the non-Markovian regime, the memory effects become significant; here we observe the emergence of BTC, signified by persistent, robust oscillations in  $m_z$ , even for smaller values of  $\omega_0/\kappa_0$ . Further, in contrast to the Markovian regime, non-Markovian dynamics is characterized by a irregular non-BTC phase for small values of  $\omega_0/\kappa_0$ . On the other hand large  $\omega_0/\kappa_0$  is associated with HO-LC phases, for non-Markovian dynamics.

As shown in Fig. 5, the value of  $\mathcal{N}$  increases monotonically as the system is driven deeper into the non-Markovian regime, characterized by smaller values of  $m$ , while it remains zero in the Markovian regime ( $m > 2\kappa_0$ ). Interestingly, increase in  $\mathcal{N}$  results in the BTC regime occurring for smaller values of  $\omega_0/\kappa_0$ , indicating the beneficial effects of information backflow for making BTC more robust against dissipation.

### III. CONCLUSION

In this work we have shown that non-Markovian dynamics can be significantly beneficial for preserving BTCs in the presence of stronger rates of dissipation, in comparison to Markovian dynamics. In the Markovian regime, BTC phase is destroyed and gets replaced by a

time-independent steady state for  $\omega_0/\kappa_0 \lesssim 1$ ; in contrast, as shown in Figs. 1 and 2, information backflow for non-Markovian dynamics can preserve time crystalline order even for  $\omega_0/\kappa_0 \lesssim 1$ . On the contrary, too small  $\omega_0/\kappa_0$  results in a irregular phase, while larger values of  $\omega_0/\kappa_0$  give rise to higher-order limit cycle dynamical phase with multiple peaks in the FFT. In order to have a deeper understanding of the dynamical phases, we have studied the QFI as a function of  $\omega_0/\kappa_0$ . Interestingly, QFI does not show any signature of HO-LC to BTC transition, which can be attributed to the absence of any phase transition between these two phases, as also signified by the limit cycle feature for both the phases. On the other hand, transition between BTC to irregular phase for small  $\omega_0/\kappa_0$  is accompanied by multiple peaks in the QFI. The same phase transition is also manifested in the behavior of the order parameter, which rises with decreasing  $\omega_0/\kappa_0$  in the ordered (BTC and HO-LC) phase, giving way to a irregular regime at the BTC - irregular phase transition point, finally showing a sharp decrease for small values of  $\omega/\kappa_0$  (see Fig. 3).

In order to understand the relation between the different dynamical phases and information backflow associated with non-Markovian dynamics, next we have considered the non-Markovianity parameter  $\mathcal{N}$ ; one can increase  $\mathcal{N}$  by decreasing  $m$ , i.e., by entering deeper inside the non-Markovian regime, as shown in Fig. 5. We have plotted the FFT peak ratio as a function of  $\mathcal{N}$  in Fig. 4. The FFT peak ratio shows irregular behavior and rises sharply with  $\mathcal{N}$  for small  $\mathcal{N}$  in the irregular regime, which changes to a smooth variation with  $\mathcal{N}$  in the BTC phase (corresponding to intermediate values of  $\mathcal{N}$ ), which changes to a sharp decrease with  $\mathcal{N}$  in the HO-LC phase (corresponding to larger values of  $\mathcal{N}$ ). This indicates the benefits of information backflow associated with non-Markovian dynamics for preserving BTC, and also raises questions regarding the relation between dynamical phases and other measures of non-Markovianity, such as quantum relative entropy [44].

Next we have plotted the phase diagram as a function of  $\omega_0/\kappa_0$  and  $m$  in Fig. 5. As observed for the discrete time crystal, the Markovian to non-Markovian transition at  $m = 2\kappa_0$  is associated with distinct change in the phase diagram. In the Markovian phase we get BTC phase only for large  $\omega_0/\kappa_0$ , while smaller values of  $\omega_0/\kappa_0$  are associated with a TISS phase. In contrast, the phase diagram shows much richer behavior in the non-Markovian regime; irregular non-BTC phase for small  $\omega_0/\kappa_0$  gets replaced by a BTC phase for intermediate values of  $\omega_0/\kappa_0$ , which further changes to HO-LC phase for larger values of  $\omega_0/\kappa_0$ . Interestingly, the transition points between the above three regimes shift towards smaller values of  $\omega_0/\kappa_0$  for smaller values of  $m$ , indicating small  $m$  to be appropriate for getting the BTC phase, if we are restricted to smaller ranges of  $\omega_0/\kappa_0$ .

Finally, we note that the studies considered here can be realized experimentally using already available technologies; non-Markovian dynamics along with measures

of non-Markovianity has been studied experimentally using quantum optical setups [31] and machine learning models [44]. On the other hand, recently BTC has been realized in atom-cavity setup [11]. Therefore we expect experimental verification of BTC phase in the presence of non-Markovian dynamics can help us to understand more about time translational symmetry breaking, and also show us ways to make BTCs more robust to dissipation.

### ACKNOWLEDGEMENTS

B.D. acknowledges support from Prime Minister Research Fellowship(PMRF). V.M. acknowledges support from Science and Engineering Research Board (SERB) through MATRICS (Project No. MTR/2021/000055).

### Appendix A: Evolution equations

The dynamics of the system can be captured by a set of closed and nonlinear equations for the average spin magnetisation, where the expectation of any operator  $\langle O \rangle$  can be calculated from the open-system Heisenberg equation, given as [9, 16],

$$\begin{aligned} \frac{d}{dt} \langle \hat{O} \rangle = i \text{Tr}([\hat{H}_b, \hat{O}] \hat{\rho}) + \frac{\kappa(t)}{2S} \text{Tr}([\hat{S}_+, \hat{O}] \hat{S}_- \\ + \hat{S}_+ [\hat{O}, \hat{S}_-]) \hat{\rho} \end{aligned} \quad (\text{A1})$$

In the thermodynamic limit, where the total spin  $N_b \rightarrow \infty$ , the equations of motion governing the time evolution of  $m_\mu$  in this limit are given by [10]:

$$\frac{dm_x}{dt} = -2\omega_z m_y m_z + \kappa(t) m_x m_z, \quad (\text{A2a})$$

$$\frac{dm_y}{dt} = 2(\omega_z - \omega_x) m_x m_z - \omega_0 m_z + \kappa(t) m_y m_z, \quad (\text{A2b})$$

$$\frac{dm_z}{dt} = \omega_0 m_y - \kappa(t) (m_x^2 + m_y^2) + 2\omega_x m_x m_y. \quad (\text{A2c})$$

These nonlinear equations couple all three components of the Bloch vector. They conserve the total magnetization norm,

$$\mathcal{N} = m_x^2 + m_y^2 + m_z^2 = 1, \quad (\text{A3})$$

which reflects the conservation of total spin magnitude in the absence of quantum fluctuations and external noise.

### Appendix B: Non-zero $\omega_x$ and $\omega_z$

To examine the behavior of the BTC phase under more general conditions, we consider the case of non-zero  $\omega_x$

and  $\omega_z$ . Our analysis reveals that in the Markovian regime characterized by strong dissipation the system relaxes into a time-independent steady state. In contrast,

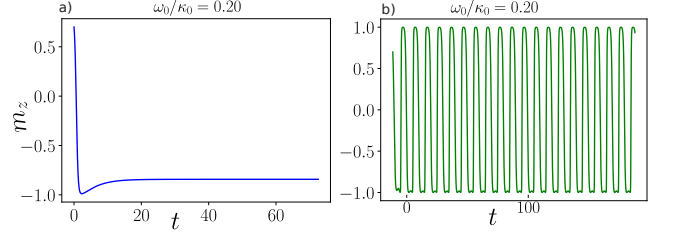


FIG. 6. Time evolution of  $m_z$  for general case where  $\omega_x = 1, \omega_z = 0.6$  (a) the Markovian regime, where  $\kappa(t) = \kappa_0$  for all  $t$ , and (b) the non-Markovian regime with modulation amplitude  $m = \kappa_0/4$ , for  $\omega_0/\kappa_0 = 0.20$ . In the Markovian case, the system reaches a time-independent steady state, whereas the non-Markovian dynamics lead to a BTC phase characterized by persistent oscillations.

in the non-Markovian regime, the system exhibits persistent oscillations indicative of the BTC phase (see Fig. 6).

### Appendix C: Non-BTC regime for very low frequency

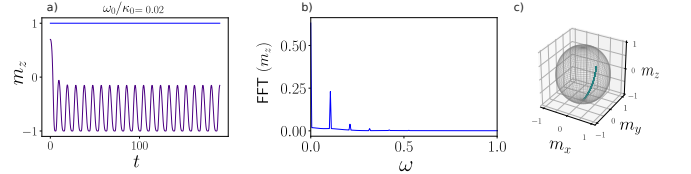


FIG. 7. Figure showing (a)  $m_z$  as a function of time, the corresponding (b) FFT and (c) the Bloch sphere representation plotted for the last 10 cycles of the BTC, in the non-Markovian regime. As shown by the Bloch sphere representation, this dynamics does not correspond to a limit cycle, and hence cannot be deemed as a BTC. Here  $m = \kappa_0/4$  and  $\omega_0/\kappa_0 = 0.02$ .

For  $\frac{\omega_0}{\kappa_0} \ll 1$ , the system exhibits periodic oscillations in the non-Markovian regime. We note that this phase is distinct from the BTC phase, as evident from the Bloch sphere representation, which shows that these oscillations do not correspond to a limit cycle (see Fig. 7).

- 
- [1] Jacek Dziarmaga. Dynamics of a quantum phase transition and relaxation to a steady state. *Advances in Physics*, 59(6):1063–1189, 2010.
  - [2] Amit Dutta, Gabriel Aeppli, Bikas K. Chakrabarti, Uma Divakaran, Thomas F. Rosenbaum, and Diptiman Sen. *Quantum Phase Transitions in Transverse Field Spin Models: From Statistical Physics to Quantum Information*. Cambridge University Press, 2015.
  - [3] Andrew D King, Sei Suzuki, Jack Raymond, Alex Zucca, Trevor Lanting, Fabio Altomare, Andrew J Berkley, Sara Ejtemaee, Emile Hoskinson, Shuiyuan Huang, Eric Ladizinsky, Allison J R MacDonald, Gaelen Marsden, Travis Oh, Gabriel Poulin-Lamarre, Mauricio Reis, Chris Rich, Yuki Sato, Jed D Whittaker, Jason Yao, Richard Harris, Daniel A Lidar, Hidetoshi Nishimori, and Mohammad H Amin. Coherent quantum annealing in a programmable 2,000 qubit ising chain. *Nature Physics*, 18(11):1324–1328, November 2022.
  - [4] Krzysztof Sacha. Modeling spontaneous breaking of time-translation symmetry. *Phys. Rev. A*, 91:033617, Mar 2015.
  - [5] Michael P. Zaletel, Mikhail Lukin, Christopher Monroe, Chetan Nayak, Frank Wilczek, and Norman Y. Yao. Colloquium: Quantum and classical discrete time crystals. *Rev. Mod. Phys.*, 95:031001, Jul 2023.
  - [6] Vedika Khemani, C. W. von Keyserlingk, and S. L. Sondhi. Defining time crystals via representation theory. *Phys. Rev. B*, 96:115127, Sep 2017.
  - [7] Soonwon Choi, Joonhee Choi, Renate Landig, Georg Kucsko, Hengyun Zhou, Junichi Isoya, Fedor Jelezko, Shinobu Onoda, Hitoshi Sumiya, Vedika Khemani, et al. Observation of discrete time-crystalline order in a disordered dipolar many-body system. *Nature*, 543(7644):221–225, 2017.
  - [8] Soham Pal, Naveen Nishad, T. S. Mahesh, and G. J. Sreejith. Temporal order in periodically driven spins in star-shaped clusters. *Phys. Rev. Lett.*, 120:180602, May 2018.
  - [9] Fernando Iemini, Angelo Russomanno, Jonathan Keeling, Marco Schirò, Marcello Dalmonte, and Rosario Fazio. Boundary time crystals. *Physical review letters*, 121(3):035301, 2018.
  - [10] Luis Fernando dos Prazeres, Leonardo da Silva Souza, and Fernando Iemini. Boundary time crystals in collective  $d$ -level systems. *Phys. Rev. B*, 103:184308, May 2021.
  - [11] Phatthamon Kongkhambut, Jim Skulte, Ludwig Mathey, Jayson Cosme G., Andreas Hemmerich, and Hans Kessler. Observation of a continuous time crystal. *Science*, 377(6606):670, 2022.
  - [12] Federico Carollo, Kay Brandner, and Igor Lesanovsky. Nonequilibrium many-body quantum engine driven by time-translation symmetry breaking. *Phys. Rev. Lett.*, 125:240602, Dec 2020.
  - [13] S. Autti, P. J. Heikkinen, J. T. Mäkinen, G. E. Volovik, V. V. Zavjalov, and V. B. Eltsov. Ac josephson effect between two superfluid time crystals. *Nature Materials*, 20(2):171–174, Feb 2021.
  - [14] Federico Carollo, Igor Lesanovsky, Mauro Antezza, and Gabriele De Chiara. Quantum thermodynamics of boundary time-crystals. *Quantum Science and Technology*, 9(3):035024, may 2024.
  - [15] Andreu Riera-Campeney, Maria Moreno-Cardoner, and Anna Sanpera. Time crystallinity in open quantum systems. *Quantum*, 4:270, May 2020.
  - [16] Zongping Gong, Ryusuke Hamazaki, and Masahito Ueda. Discrete time-crystalline order in cavity and circuit qed systems. *Phys. Rev. Lett.*, 120:040404, Jan 2018.
  - [17] Hans Keßler, Phatthamon Kongkhambut, Christoph Georges, Ludwig Mathey, Jayson G Cosme, and Andreas Hemmerich. Observation of a dissipative time crystal. *Physical Review Letters*, 127(4):043602, 2021.
  - [18] Giulia Piccitto, Matteo Wauters, Franco Nori, and Nathan Shammah. Symmetries and conserved quantities of boundary time crystals in generalized spin models. *Phys. Rev. B*, 104:014307, Jul 2021.
  - [19] Mrutyunjaya Sahoo, Rahul Ghosh, Bandita Das, Shishira Mahunta, Bodhaditya Santra, and Victor Mukherjee. Generating discrete time crystals through optimal control, 2025.
  - [20] Bihui Zhu, Jamir Marino, Norman Y Yao, Mikhail D Lukin, and Eugene A Demler. Dicke time crystals in driven-dissipative quantum many-body systems. *New Journal of Physics*, 21(7):073028, jul 2019.
  - [21] Bandita Das, Noufal Jaseem, and Victor Mukherjee. Discrete time crystals in the presence of non-markovian dynamics. *Phys. Rev. A*, 110:012208, Jul 2024.
  - [22] Parvinder Solanki, Midhun Krishna, Michal Hajdušek, Christoph Bruder, and Sai Vinjanampathy. Exotic synchronization in continuous time crystals outside the symmetric subspace. *Phys. Rev. Lett.*, 133:260403, Dec 2024.
  - [23] Parvinder Solanki and Fabrizio Minganti. Chaos in time: A dissipative continuous quasi time crystals, 2024.
  - [24] Heinz-Peter Breuer and Francesco Petruccione. *The Theory of Open Quantum Systems*. Oxford University Press, 01 2007.
  - [25] D. F. Walls, P. D. Drummond, S. S. Hassan, and H. J. Carmichael. Non-equilibrium phase transitions in cooperative atomic systems. *Progress of Theoretical Physics Supplement*, 64:307–320, 02 1978.
  - [26] Heinz-Peter Breuer, Elsi-Mari Laine, Jyrki Piilo, and Bassano Vacchini. Colloquium: Non-markovian dynamics in open quantum systems. *Rev. Mod. Phys.*, 88:021002, Apr 2016.
  - [27] Wei-Min Zhang, Ping-Yuan Lo, Heng-Na Xiong, Matisse Wei-Yuan Tu, and Franco Nori. General non-markovian dynamics of open quantum systems. *Phys. Rev. Lett.*, 109:170402, Oct 2012.
  - [28] Victor Mukherjee, Vittorio Giovannetti, Rosario Fazio, Susana F Huelga, Tommaso Calarco, and Simone Montangero. Efficiency of quantum controlled non-markovian thermalization. *New Journal of Physics*, 17(6):063031, 2015.
  - [29] Dariusz Chruściński and Sabrina Maniscalco. Degree of non-markovianity of quantum evolution. *Phys. Rev. Lett.*, 112:120404, Mar 2014.
  - [30] Heinz-Peter Breuer, Elsi-Mari Laine, and Jyrki Piilo. Measure for the degree of non-markovian behavior of quantum processes in open systems. *Phys. Rev. Lett.*, 103:210401, Nov 2009.
  - [31] Gerhard Rempe, Herbert Walther, and Norbert Klein. Observation of quantum collapse and revival in a one-atom maser. *Phys. Rev. Lett.*, 58:353–356, Jan 1987.

- [32] Bogna Bylicka, Markus Johansson, and Antonio Acín. Constructive method for detecting the information backflow of non-markovian dynamics. *Phys. Rev. Lett.*, 118:120501, Mar 2017.
- [33] Yun-Yi Hsieh, Zheng-Yao Su, and Hsi-Sheng Goan. Non-markovianity, information backflow, and system-environment correlation for open-quantum-system processes. *Phys. Rev. A*, 100:012120, Jul 2019.
- [34] Fernando Iemini, Rosario Fazio, and Anna Sanpera. Floquet time crystals as quantum sensors of ac fields. *Phys. Rev. A*, 109:L050203, May 2024.
- [35] Dominic Gribben, Anna Sanpera, Rosario Fazio, Jamir Marino, and Fernando Iemini. Boundary time crystals as AC sensors: Enhancements and constraints. *SciPost Phys.*, 18:100, 2025.
- [36] Victor Montenegro, Marco G. Genoni, Abolfazl Bayat, and Matteo G. A. Paris. Quantum metrology with boundary time crystals. *Communications Physics*, 6(1):304, Oct 2023.
- [37] Dominic Gribben, Anna Sanpera, Rosario Fazio, Jamir Marino, and Fernando Iemini. Boundary time crystals as ac sensors: Enhancements and constraints. *SciPost Physics*, 18(3):100, 2025.
- [38] Michael A. Nielsen and Isaac L. Chuang. *Quantum Computation and Quantum Information: 10th Anniversary Edition*. Cambridge University Press, 2010.
- [39] Federico Carollo and Igor Lesanovsky. Exact solution of a boundary time-crystal phase transition: Time-translation symmetry breaking and non-markovian dynamics of correlations. *Phys. Rev. A*, 105:L040202, Apr 2022.
- [40] Robert Mattes, Igor Lesanovsky, and Federico Carollo. Entangled time-crystal phase in an open quantum light-matter system. *Phys. Rev. A*, 108:062216, Dec 2023.
- [41] Michael J. W. Hall, James D. Cresser, Li Li, and Erika Andersson. Canonical form of master equations and characterization of non-markovianity. *Phys. Rev. A*, 89:042120, Apr 2014.
- [42] Ángel Rivas, Susana F Huelga, and Martin B Plenio. Quantum non-markovianity: characterization, quantification and detection. *Reports on Progress in Physics*, 77(9):094001, aug 2014.
- [43] Jyrki Piilo, Sabrina Maniscalco, Kari Härkönen, and Kalle-Antti Suominen. Non-markovian quantum jumps. *Phys. Rev. Lett.*, 100:180402, May 2008.
- [44] K. Goswami, C. Giarmatzi, C. Monterola, S. Shrapnel, J. Romero, and F. Costa. Experimental characterization of a non-markovian quantum process. *Phys. Rev. A*, 104:022432, Aug 2021.